The mechanism of the catalysis of the Claisen rearrangement of chorismate to prephenate by the chorismate mutase from *Bacillus subtilis*. A molecular mechanics and hybrid quantum mechanical/molecular mechanical study

Mark M. Davidson, Ian R. Gould † and Ian H. Hillier *

Chemistry Department, University of Manchester, Manchester, UK M13 9PL

The role of the active site of the chorismate mutase from *Bacillus subtilis* in catalysing the Claisen rearrangement of chorismate to prephenate is studied computationally using both molecular mechanics and a hybrid quantum mechanical/molecular mechanical method. Structures along the pathway calculated at the HF/6-31G* level are docked into the active site and reveal that the hydrogen bonding interactions reflect the changing geometry and electronic structure of the substrate. In particular the interactions are maximal close to the transition state and lead to a barrier lowering greater than that needed to produce the observed rate acceleration in line with conclusions that the chemical transformation is not the rate determining process.

Introduction

The Claisen rearrangement of chorismate (**1**) to prephenate (**2**) is a unique pericyclic reaction, occurring in solution and being catalysed by chorismate mutase enzymes[1] and catalytic antibodies.[2,3] Chorismate mutase is involved in the shikimate pathway which is responsible for biosynthesis of aromatic amino acids.[1,4] Since this enzyme exists in bacteria, fungi and higher plants, it is a potential target for the design of antibiotics, herbicides and antifungal agents.

The importance of chorismate mutase is not limited to it being the only known natural enzyme to catalyse a pericyclic reaction. For a number of reasons this enzyme presents a unique opportunity for theoretical study. The rearrangement occurring in the active site of the enzyme is likely to be similar to the reaction occurring independent of the enzyme and so direct comparison between catalysed and uncatalysed rearrangements is possible,[5-7] a rare situation for enzyme catalysed reactions. Rearrangement of chorismate by the enzyme also occurs with no direct involvement of the enzyme in the reaction (*i.e.* no covalent bonds are formed between enzyme and substrate) and therefore the catalytic effect presumably arises from non-bonded interaction between the enzyme and substrate. The difficulty of modelling covalent bonding between enzyme and substrate is thus removed. The relatively small size of the substrate, chorismate, makes it possible to study the rearrangement by moderate level *ab initio* calculations. Such calculations have recently been reported for the rearrangement both of chorismate[8,9] and related analogues,[10,11] in the gas phase. In addition, for a substrate the size of chorismate it is possible to accurately model the effect of the environment on the rearrangement pathway, which is central to understanding the mode of action of the enzyme.[8] We here describe calculations of the interaction between structures on the rearrangement pathway of (**1**)→(**2**) and the active site of the enzyme chorismate mutase. These are first carried out using classical force fields in order to focus on the important features of the interaction. The model is then refined by use of a hybrid quantum mechanical (QM)/molecular mechanical (MM) approach to obtain a quantitative reaction path for the enzyme catalysed reaction.

† Present Address: Chemistry Department, Imperial College of Science and Medicine, South Kensington, London, UK SW7 2AY.

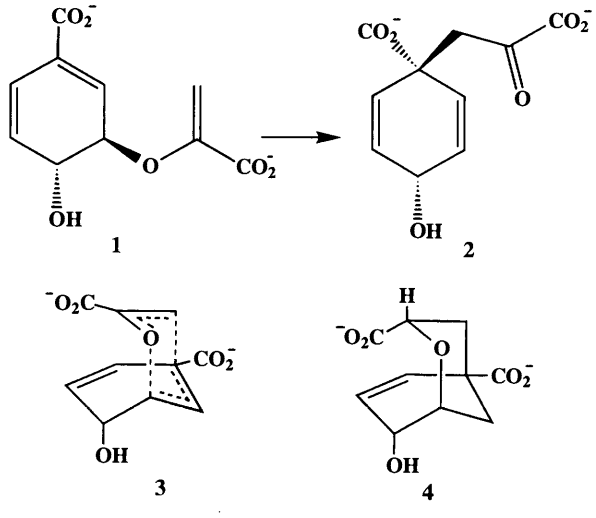

Any theoretical study of enzyme catalysis usually requires a structure of the enzyme from X-ray crystallography. The structure of chorismate mutase for this current study was taken from the X-ray crystal coordinates of chorismate mutase from *Bacillus subtilis*.[5,6] However, X-ray crystal structures also exist for a genetically engineered mutase derived from the *Escherichia coli* 'P' protein,[12] a chorismate mutase from yeast (*Sacchaomyces cerevisiae*)[13] and a catalytic antibody with chorismate mutase activity.[7] Although all these proteins have different active site structures, they presumably all employ a similar catalytic mechanism to accelerate the rearrangement of chorismate. The work presented herein on the study of chorismate mutase from *Bacillus subtilis* will probably be the first of many more theoretical studies of chorismate mutase and derivatives.

Molecular mechanical model of substrate–enzyme interactions

Computational details

We first describe calculations to investigate the interactions that the stationary structures on the chorismate to prephenate potential energy surface have with the active site of chorismate mutase. Here the interactions are modelled using appropriate

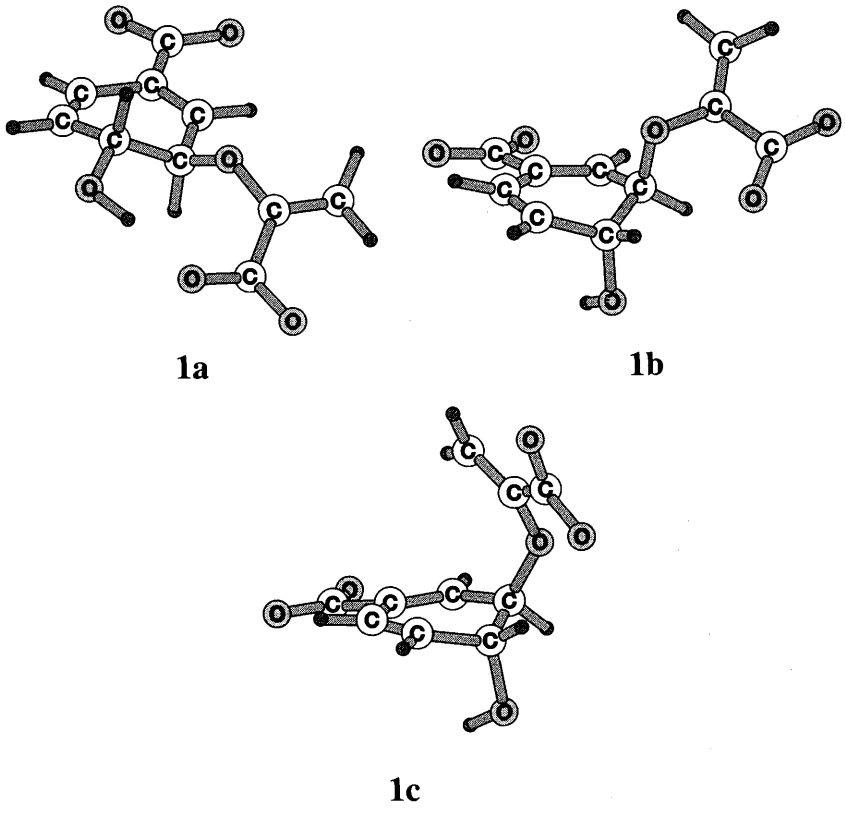

Fig. 1 Minimum energy structures for chorismate

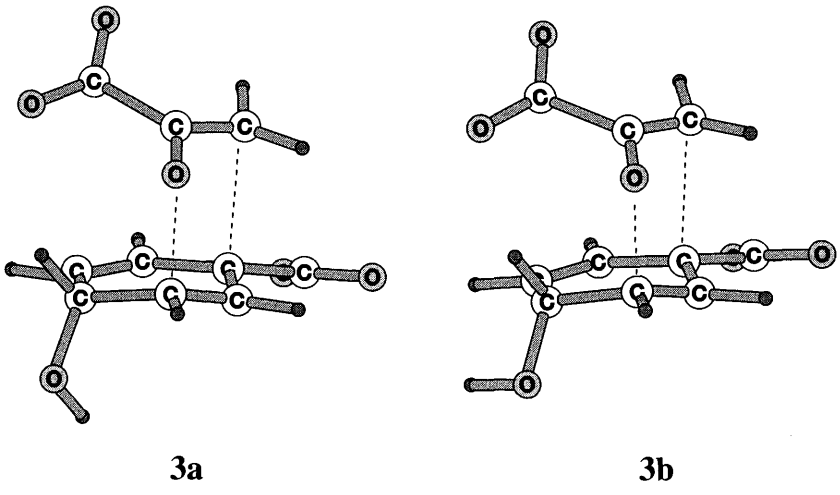

Fig. 2 Transition state structures (**3**) with hydroxy orientated OH in (**3a**) and OH out (**3b**)

force fields. We first discuss the structure of the reactant, chorismate (**1**), product, prephenate (**2**) and the transition state (**3**). These structures were obtained and characterised by calculation of the harmonic frequencies at the Hartree–Fock (HF) *ab initio* level using a 6-31G* basis, and the program GAUSSIAN92[14] on the Fujitsu VPX 240/10 of the Manchester Computing Centre. There are important aspects of the conformation of these species, particularly the reactant and transition state, that need to be considered. The chorismate dianion (**1**) can adopt several conformations and these have been studied in solution by Copley and Knowles, using NMR.[15] We have located and characterised as minima the structures discussed by Copley and Knowles. These structures can be labelled either diequatorial or diaxial depending on the position of the ether and hydroxy oxygen atoms with respect to the cyclohexadienyl ring. The most stable structure is found to be the diequatorial conformation (**1a**) (Fig. 1). The stability of this structure is due to the intramolecular hydrogen bond formed between the ring hydroxy group and the side-chain carboxylate group. Higher energy structures have been found for the diaxial conformation. The lowest energy diaxial structure (**1b**) has the enolpyruvyl moiety positioned to avoid steric repulsion with the cyclohexadienyl ring, in contrast to the higher energy diaxial conformer (**1c**) where such steric interaction can be seen to be present. However, it is this latter diaxial conformer that has a similar structure to the transition state (**3**) and is the conformer from which the pericyclic rearrangement must ensue. This conformer is also believed to be selectively bound by the enzyme, chorismate mutase.[5–7]

We turn now to the calculated structure of the transition state (Fig. 2). The transition state involved in the rearrangement has little of the conformational freedom of the reactant except for the conformational orientation of the ring hydroxy group. We have characterised two transition state structures. The more energetically favourable one [by 4.0 kcal mol^{-1} (1 cal = 4.189 J)] has the hydroxy group directed towards the ring (–OH in) (**3a**) rather than away from the ring (–OH out) (**3b**). The reactant conformer **1c** which leads to the transition state

Table 1 ESP charges of chorismate, transition state and prephenate used for docking in active site of chorismate mutase

Atom	Chorismate	Transition state	Prephenate
C_1	−0.58	−0.61	−0.24
C_2	0.22	0.33	0.49
O_3	−0.44	−0.58	−0.62
C_4	0.20	0.33	−0.39
C_5	−0.31	−0.71	−0.15
C_6	−0.01	0.53	0.28
C_7	0.01	−0.52	−0.25
C_8	−0.41	0.09	−0.24
C_9	0.46	0.22	0.65
O_{10}	−0.73	−0.75	−0.76
C_{11}	0.83	0.78	0.84
O_{12}	−0.81	−0.81	−0.82
O_{13}	−0.83	−0.82	−0.83
C_{14}	0.84	0.84	0.77
O_{15}	−0.82	−0.84	−0.81
O_{16}	−0.82	−0.83	−0.80

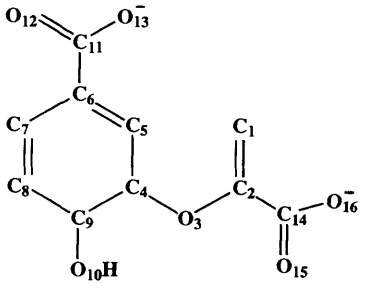

Atom labelling

3a, this latter structure, and the corresponding structure of prephenate (**2**) having the side arm positioned over the cyclohexadiene ring, were then docked in the active site of the enzyme.

The starting point for this MM study is the X-ray structure of chorismate mutase from *Bacillus subtilis*,[5,6] with Bartlett's transition state analogue (**4**)[16] bound into each of the three active sites of this trimeric enzyme. This structure from which the MM model was built has three equivalent binding pockets but only one of these is considered in our substrate binding studies. Therefore, the other two binding sites were filled with MM models of Bartlett's inhibitor as found in the X-ray crystal structure of this enzyme. Any future reference to an active site will correspond to the one used for docking in the substrates. AMBER[17] was used to build and optimise structures of the enzyme with the substrates (**1c**, **2** and **3a**) docked in the binding pocket. The united-atom force field[18] was used to represent the bulk of the enzyme and the all-atom force field[19] was chosen for the catalytically important residues, which form the active site, where hydrogen bonding is important. This includes residues within 12 Å of the centre of the active site.

The orientation of Bartlett's inhibitor bound in the active site of chorismate mutase, determined from X-ray crystallography,[5,6] was used as a template to align each of the substrates (**1**, **2** and **3**) in the binding pocket. Some conformational freedom of these species was permitted to maximise the interaction of the ring –OH group with the Glu78 residue of the active site. Atom centred partial charges were required for each of the substrates and these were obtained from HF/6-31G* *ab initio* wavefunctions, following the method of Singh and Kollman.[20] This method produces a set of atom centred partial charges (Table 1) which reproduce an *ab initio* calculated electrostatic potential (ESP charges). Energy minimisation was then carried out to refine the docking of each of the structures **1**, **2** and **3** within the enzyme active site. During the MM minimisation the substrates remained fixed in their *ab initio* optimised structures and only residues within 12 Å of the active site were allowed to move. A 12 Å non-bonded cutoff was used. Minimisation was carried out using the steepest descent method for 200 steps followed by conjugate gradient minimisation to an RMS energy gradient of 0.1 kcal mol^{-1} $Å^{-1}$. In all, a total of approximately 5000 steps of minimisation were required for each substrate.

Computational results and discussion

We show in Fig. 3 schematic diagrams of *ab initio* optimised structures of the substrates and of Bartlett's transition state analogue (**4**) taken from the X-ray structure of chorismate mutase with this inhibitor bound in the active site.[5,6] The similarity between the calculated transition state structure (**3**) and the experimental crystal structure of Bartlett's analogue (**4**) is immediately apparent. Overlapping the two structures (**3**) and (**4**) gave an RMS deviation of the heavy atom positions of only 0.32 Å showing the high degree of similarity between the two structures. The concept that the active sites of enzymes are structurally and electrostatically complimentary to the substrate in its activated transition state is well established and has led to the design of many inhibitors based on proposed transition state structures.[21–23] Bartlett's transition state analogue (**4**) is the most potent inhibitor of chorismate mutase activity known. Our results show the similarity between this inhibitor and our calculated transition state structure and thus have demonstrated the value of the transition state analogue concept.

The initial manual docking of the transition state (**3**) and prephenate (**2**) into the active site was straightforward. The heavy atom positions in the substrate molecules mapped closely to equivalent positions in the template inhibitor molecule, allowing these substrates to fit tightly in the active site. However, chorismate itself did not fit so closely into the active site which caused the ring carboxylate group to closely approach the side of the entrance to the active site, unlike the other two structures where this group pointed directly out of the entrance. The –OH group in each of the manually docked structures was rotated from its optimal *in vacuo* position to maximise its interaction with Glu78.

The calculated partial charges for the three substrate structures, including the –OH rotation (Table 1) show as expected little change in the values calculated for the ring carboxylate, ring hydroxy and side chain carboxylate between the three structures, since these groups are not directly involved in the reaction but are responsible for tight binding of the substrate during the rearrangement. All other charges vary to some degree reflecting the change in geometric and electronic structure during the rearrangement.

Molecular mechanics minimisation of the manually docked structures resulted in all major interactions found experimentally[5] between Bartlett's inhibitor and chorismate mutase, also being found in the predicted structures (Fig. 4). To verify that no major rearrangement of the enzyme had occurred the resulting structures from the MM minimisations were compared with the original *Bacillus subtilis* X-ray structure. The RMS deviations from the X-ray structure were 0.61, 0.56 and 0.57 Å for chorismate, transition state and prephenate, respectively, considering the main chain protein atoms. More importantly, the relative positions of key residues (Arg90, Arg7, Tyr108, Glu78 and Cys75) were after minimisation, in each of the cases very similar to those in the X-ray structure. Orientation of the substrates in the active site produces the greatest number of contacts to the side chain carboxylate and ring hydroxy groups. The only slight difference between experiment and our structures is that the interaction of Cys75 with the substrates occurs with the main chain amide (NH) of this residue rather than the side chain SH, as was proposed from the structural studies.[5] As judged from the calculated structures (Fig. 4) the strongest hydrogen bonding interactions were found to occur between the enzyme and the side arms of the substrates (atoms O_3, O_{15} and O_{16}). This situation is not unexpected as it

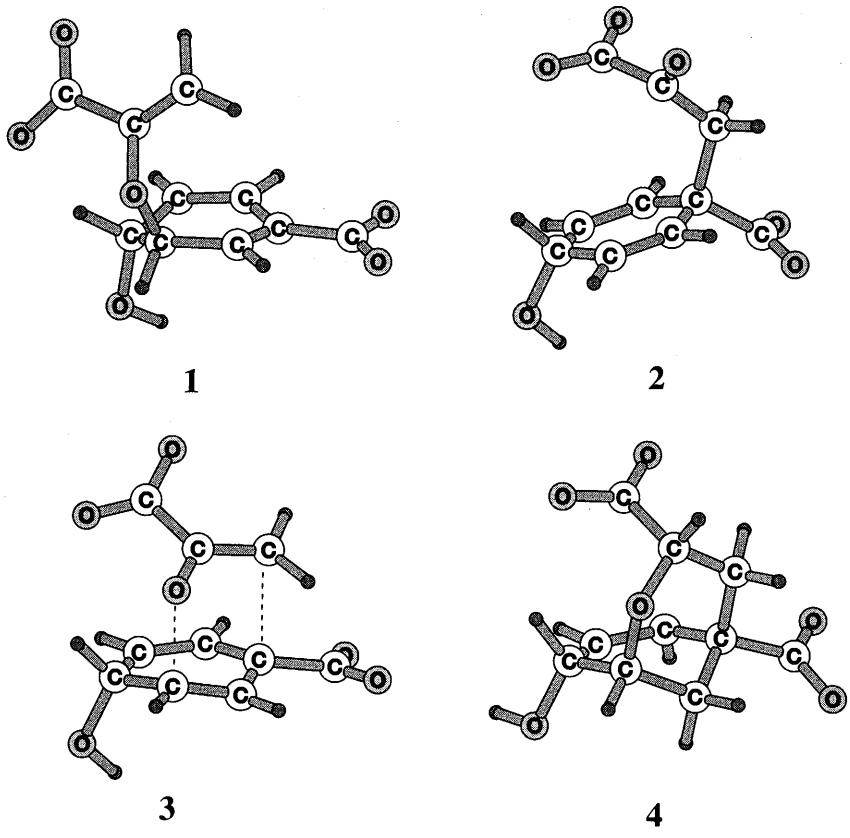

Fig. 3 Optimised structures of chorismate (**1**), prephenate (**2**), transition state (**3**) and Bartlett's inhibitor (**4**)

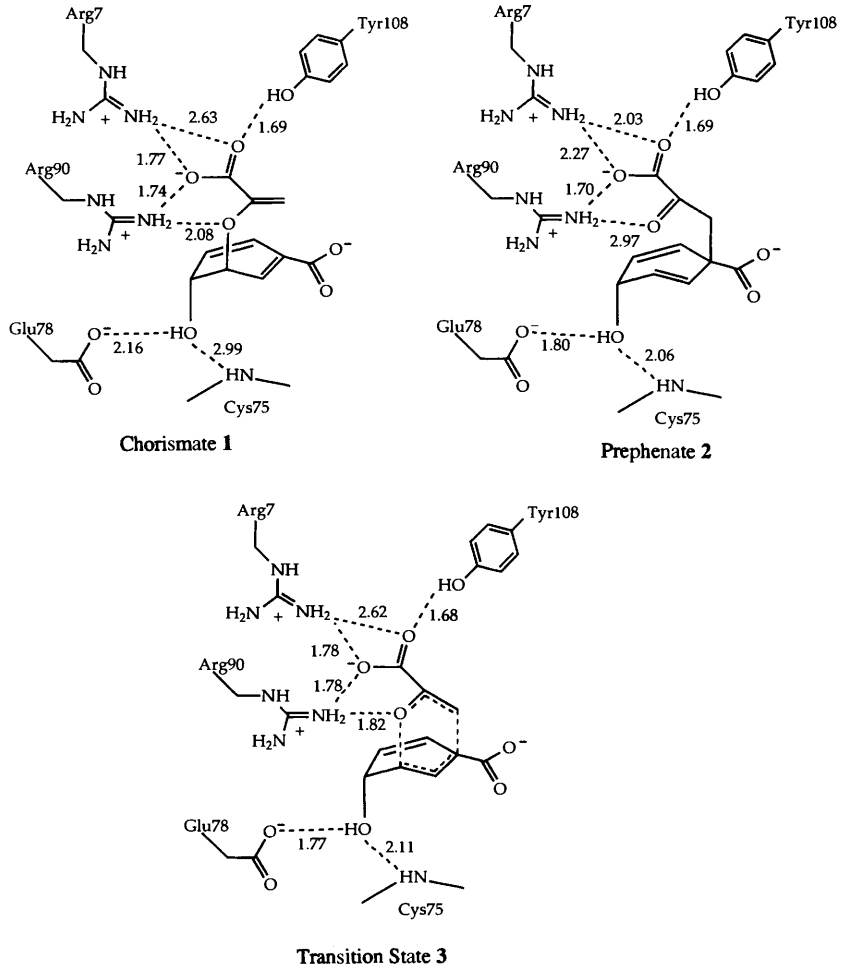

Fig. 4 Predicted substrate–active site structures

Table 2 Substrate–enzyme interaction energies (kcal mol^{-1})

	Electrostatic	van der Waals[a]
Chorismate (**1**)	−11.9	−17.0
Transition state (**3**)	−37.3	−19.2
Prephenate (**2**)	−32.8	−19.8

[a] Including hydrogen-bond term.

has been suggested that chorismate mutases energetically select the requisite diaxial conformation of the flexible chorismate molecule with the side arm positioned over the cyclohexadiene ring. The relatively poor fitting of chorismate in the active site is reflected in the predicted intermolecular interactions. Weaker hydrogen bonds are formed between chorismate's hydroxy group and both Glu78 and Cys75 compared to the much stronger interactions formed to both the transition state and prephenate. Furthermore, the poor fit of chorismate results in the ring carboxylate of chorismate forming two relatively weak hydrogen bonds with Lys176 and Ala175 of 2.18 and 2.14 Å, respectively, at the entrance to the active site. The transition state and prephenate have this group pointing out of the entrance.

From the calculated structures (Fig. 4) we conclude that a much stronger hydrogen bond is formed between Arg90 and the ether oxygen (O_3) of the transition state compared to that of chorismate. Furthermore, this interaction becomes much weaker for prephenate in the active site, reflecting the structure of the product where on formation of the carbonyl group, this group rotates away from the cyclohexadiene ring (as shown in Fig. 3) breaking the hydrogen bond with the Arg90 residue. The prephenate-bound structure is consistent with FTIR studies[24] which indicate that there is no polarisation of the carbonyl group of prephenate by the enzyme in line with our calculated interaction structure. The weakening of the Arg90 with the carbonyl O_3 in the prephenate case results in an increased interaction of Arg7 with the side chain carboxylate. NMR studies[25] have shown that, under saturating conditions, dissociation of prephenate from the active site is the rate-limiting step of the reaction. Upon examination of our predicted prephenate-bound enzyme structure it is evident that prephenate forms many strong interactions with the enzyme. Thus, the tight fit of prephenate in the enzyme could retard its diffusion out of the active site.

In Table 2 we show the interaction energies contributing to the binding of **1**, **2** and **3** in the active site of the enzyme. These values were calculated for the full trimer structure of the enzyme and reflect the nature of the interactions described above. It is clear that the electrostatic contributions are dominant. In particular the large electrostatic interaction with the transition state structure reflects the enzyme's geometric and electrostatic complimentarity to the transition structure. From our calculated structures (Fig. 4) a major source of the preferential electrostatic stabilisation of the transition state arises from enhanced hydrogen bonding between the ether oxygen (O_3) and the Arg90 residue. This is analogous to the origin of the enhancement of the rate of the Claisen rearrangement of allyl vinyl ether in water, previously discussed by us,[26] where again enhanced hydrogen bonding to the transition state was responsible for acceleration of this rearrangement. The tight fitting of the product in the enzyme is also shown in the calculated interaction energies (Table 2).

Thus, in accord with conventional ideas concerning enzyme catalysis,[27] the transition state is found to interact the strongest with the enzyme leading to electrostatic stabilisation of the transition structure and to a lowering of the barrier for this rearrangement. No account has been taken in this study of solvation as no important catalytic water molecules were observed in structural studies of Bartlett's inhibitor bound in chorismate mutase.[5,6] Furthermore, solvent is usually included around a protein to stop unrealistic movement of mobile side chains. However this present study is only addressing the structure of the active site and interaction of active site residues with substrates so that it was felt unnecessary to include solvent.

This molecular mechanics study has given valuable insight into the important interactions between chorismate mutase and various structures representing stationary points on the chorismate to prephenate rearrangement, including the transition state. However, for a more complete description of the transition state at the active site and also to include the changes in electronic structure along the reaction pathway a quantum mechanical approach is needed. This may be achieved by using a hybrid QM/MM method where the substrate is treated quantum mechanically and the surrounding field of the enzyme is treated molecular mechanically and the two systems are coupled by electrostatic and van der Waals interactions. The application of such a hybrid approach to the enzyme catalysed reaction is now described.

Hybrid QM/MM study of the reaction pathway

Computational details

Hybrid QM/MM methods to model enzyme catalysis have been described using both *ab initio*[28,29] and semiempirical[30–32] QM methods. We here employ the GAUSSIAN92[14] QM program linked to the AMBER[17] MM program *via* the GAUSSIAN link structure. Geometry optimisation was carried out using the standard procedures within the GAUSSIAN program. Since there are no covalent interactions between the substrate and enzyme, the somewhat arbitrary procedures adopted to treat junction atoms are not needed here.

Firstly, reaction path following was performed to generate a gas phase pathway for the chorismate to prephenate rearrangement. Starting from the gas phase *ab initio* transition state structure (**3a**) an intrinsic reaction coordinate (IRC) calculation[33] was carried out to generate structures along the pathway to reactant (**1c**) and product (**2**). Intermediate structures along the rearrangement pathway were then docked into the active site of chorismate mutase, following the same procedure as described in the previous section which was used to dock in the reactant, transition state and product. Energy evaluations were performed along the reaction pathway within the enzyme, using the hybrid QM/MM method. Here the QM motif consisted of the substrate represented at the Hartree–Fock or MP2 levels using a 6-31G* basis, and the enzyme was treated molecular mechanically using the AMBER force field. A more refined model would include the important active site residues in the QM treatment. However, it is not clear that the increased computational expense would be justified. In the hybrid QM/MM approach the QM substrate interacts with the enzyme *via* the formal MM atomic charges of the enzyme (included in the one-electron Hamiltonian) and by the van der Waals forces. The whole trimeric enzymic system was considered molecular mechanically. In addition optimisation of the transition state (**3a**) within the enzyme active was carried out using the hybrid QM/MM method, although no characterisation of the stationary structure was performed. However, since little geometric variation from the gas phase structure resulted, we are confident that our structure does indeed correspond to a transition state.

Computational results and discussion

The geometry of the transition state, in the active site of chorismate mutase, optimised using the hybrid QM/MM method is given in Table 3 and is compared to the gas phase optimised structure of the transition state. Significant, though small, structural changes are induced by the enzyme. Binding of the transition state in the enzyme results in more bond breaking (C_4–O) and less bond formation (C_1–C_6) than in the gas phase. A similar situation was predicted for the Claisen rearrangement

Table 3 Calculated bond lengths (Å) of transition state in gas phase and in enzyme active site

Structure[a]	Gas phase	Enzyme (QM/MM)
C_1–C_2	1.384	1.349
C_1–C_6	2.388	2.548
C_2–O	1.270	1.287
C_4–O	1.987	2.041
C_4–C_5	1.381	1.396
C_5–C_6	1.386	1.370
C_6–C_7	1.479	1.473
C_7–C_8	1.324	1.322
C_8–C_9	1.501	1.499
C_9–C_4	1.512	1.520

[a] Atom labelling given in Table 1.

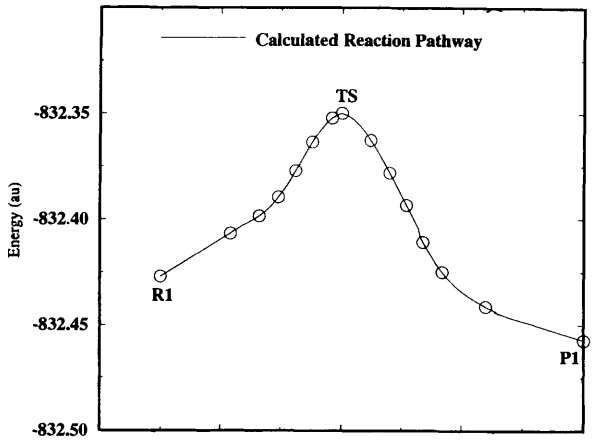

Fig. 5 Calculated reaction pathway from chorismate (R1) to prephenate (P1)

of allyl vinyl ether in aqueous media.[26,34] The binding motif between the QM/MM optimised transition state structure and the binding pocket remains essentially the same as the initial docked transition state structure with no relaxation of structure (Fig. 4). The only significant difference is that the ring carboxylate group has rotated slightly to form a new hydrogen bond with Arg116. Such an interaction between the ring carboxylate of Bartlett's inhibitor (**4**) and Arg116 is observed in a number of the binding sites in the enzyme as determined from X-ray crystallography.[5] The Arg116 residue is part of the C-terminal tail of the enzyme which is known to play a part in binding of substrates within the active site and the interaction between this residue (Arg116) and the ring carboxylate group may be part of the mechanism whereby the C-terminal tail facilitates tight binding of substrates.

We conclude that although the transition state does change its structure to some extent in the enzyme active site, the gas phase structure is considered a good approximation. Thus, a study of the whole reaction pathway, using our gas phase structures is considered to be of considerable value, particularly bearing in mind the computational cost of optimising the whole pathway within the active site.

The calculated reaction pathway is shown in Fig. 5. 15 of these structures, including the two minima, R1 (reactant) and P1 (product), and transition state (TS) were selected to be used to calculate the effect of the enzyme on the reaction pathway and these are the circled points in this figure. After manual docking of each of these structures into the enzyme, including rotation of the hydroxy so as to maximise its interaction with Glu78, molecular mechanics minimisation of the surrounding enzyme structure was carried out as before. The hydrogen bond interactions resulting from these calculations are summarised in Table 4. It can be seen that generally strong hydrogen bonding interactions are maintained throughout the reaction path. However, the hydrogen bond between Arg90 and O_3 (**A**) increases in strength as the reaction proceeds from R1 to the transition state (TS). Also, this hydrogen bond is actually broken between structure P2 and P1, resulting from the rotation of the newly formed carbonyl group in the product structure (Fig. 4). The decrease in the hydrogen bond at C between P2 and P1 is accompanied by the formation of a new hydrogen bond between Arg7 and O_{16} of 2.03 Å as shown in Fig. 4.

The energies along the reaction pathway, calculated by the hybrid QM/MM method are displayed in Fig. 6. Here the gas phase energetics are compared with those at the enzyme active site, both calculated at the HF level. The corresponding results obtained at the MP2 level are shown in Fig. 7. At the HF level the rearrangement R1→P1 in the gas phase, relative to R1 shows a large barrier of 49.3 kcal mol^{-1} (Fig. 6). We have shown that for the Claisen rearrangement of allyl vinyl ether, the barrier at the HF/6-31G* level is over estimated by about 16 kcal mol^{-1}.[35] The hybrid QM/MM calculation predicts a lower barrier (24.8 kcal mol^{-1}) at the active site of chorismate mutase. In addition, a shallow minimum is found to occur at the initial stages of the rearrangement in the enzyme and results from the stronger binding of R2 than R1 in the active site. In the gas phase structure R2 is higher in energy than R1 but has its side arm compressed towards the cyclohexadiene ring and has a stretched C_4–O bond, leading to a structure more like the transition state involved in the rearrangement. The corresponding increased binding energy results in the enzyme forming a enzyme–substrate complex with this structure (R2) rather than structure R1.

The calculated barriers in the enzyme (R2→TS) and in the gas phase (R1→TS) lead to a barrier lowering due to the enzyme of 24.5 kcal mol^{-1}, a value considerably greater than the barrier lowering of between 4.9 and 8.9 kcal mol^{-1} inferred from the observed rate enhancement of 10^6 compared to that in aqueous media.[36] However, our calculated lowering is relative to the gas phase. The barrier lowering of the rearrangement of allyl vinyl ether due to hydration has been determined to be 3.5–4.7 kcal mol^{-1}[37,38] and therefore our predicted barrier lowering is still substantially greater than the experimental value. This situation is not at odds with experiment as it has been concluded that the chemical rearrangement is not the rate limiting step. Therefore our large barrier lowering is quite consistent with experiment. The barrier to the rearrangement in the enzyme calculated at the HF/6-31G* level is 24.8 kcal mol^{-1} but by reference to the case of allyl vinyl ether this value is over estimated by about 16 kcal mol^{-1}.[35] Thus, a barrier to the enzymic rearrangement of about 9 kcal mol^{-1} is predicted.

We now discuss the barrier calculated at the MP2 level (Fig. 7). The gas phase rearrangement R1→P1 again shows a barrier, although it is significantly reduced compared to the value at the HF level. This is expected as the barrier to the rearrangement of allyl vinyl ether calculated at the MP2 level is more in line with experiment than is the HF value, being underestimated by 7 kcal mol^{-1}.[35] The lower curve in Fig. 7 again illustrates the stabilisation of the transition state within the enzyme. Again an initial dip in the reaction pathway is observed, but the pathway is relatively flat after this leading to a slight barrier to rearrangement close to structure P7. The energy then decreases to a very stable product–enzyme complex. From these curves we obtain a barrier lowering due to the enzyme of 13.8 kcal mol^{-1}, again greater than the experimental barrier lowering. The absolute barrier to the rearrangement in the enzyme calculated at the MP2/6-31G* level is 6.4 kcal mol^{-1} but by comparison to the case of allyl vinyl ether it is probably underestimated by about 7 kcal mol^{-1}.[35] In common with the HF results this gives an absolute barrier to the enzymic rearrangement of chorismate of between 9 and 13 kcal mol^{-1}.

Table 4 Hydrogen bond interaction (Å) between structures along the reaction pathway and chorismate mutase

	A	B	C	D	E	F
R1	2.08	1.74	1.77	1.69	2.16	2.99
R2	1.90	1.79	1.77	1.69	1.76	2.96
R3	1.90	1.82	1.76	1.68	1.75	3.09
R4	1.90	1.76	1.93	1.68	1.78	2.04
R5	1.86	1.77	1.77	1.68	1.75	2.05
R6	1.84	1.78	1.81	1.68	1.76	2.20
R7	1.83	1.78	1.78	1.68	1.76	2.20
TS	1.82	1.78	1.78	1.68	1.77	2.11
P7	1.82	1.80	1.77	1.69	1.76	2.39
P6	1.80	1.86	1.76	1.69	1.79	2.10
P5	1.81	1.82	1.77	1.69	1.77	2.18
P4	1.81	1.81	1.78	1.69	1.78	2.14
P3	1.81	1.80	1.80	1.69	1.79	2.07
P2	1.82	1.80	1.80	1.69	1.85	2.50
P1	2.97	1.70	2.27	1.69	1.79	2.06

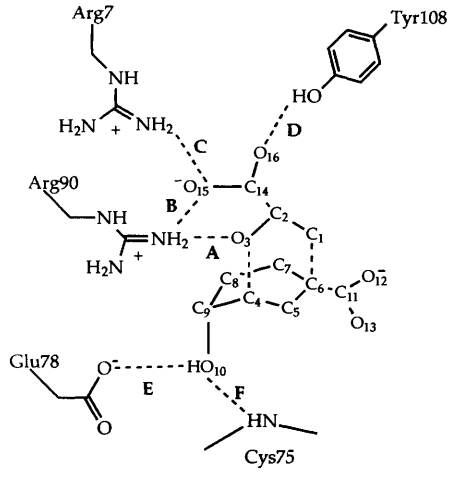

Definition of interaction distances

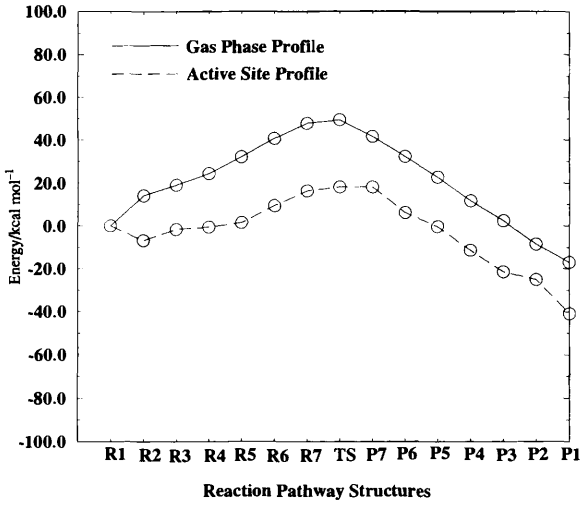

Fig. 6 The potential surface of the chorismate rearrangement (R1→P1) in the gas phase and in the enzyme calculated at the HF/6-31G* level

Conclusions

We have identified the major interactions between structures on the rearrangement pathway of chorismate to prephenate and the active site of chorismate mutase to be hydrogen bonding in nature. These interactions reflect the changing electronic and geometric structures along the pathway and are maximal close to the transition state. The predicted barrier lowering due to these interactions is greater than that needed to produce the observed enhancement of the reaction rate observed experimentally, in line with the conclusion that the chemical transformation is not the rate determining process.

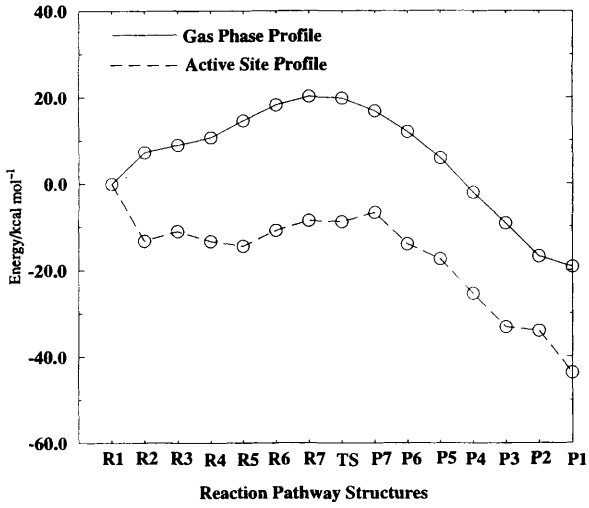

Fig. 7 The potential surface of the chorismate rearrangement (R1→P1) in gas phase and in the enzyme calculated at the MP2/6-31G* level

Acknowledgements

We thank EPSRC and Fujitsu Systems (Europe) Ltd. for support of this research.

References

1 E. Haslam, *Shikimic Acid: Metabolism and Metabolites*, Wiley, Chichester, 1993.
2 D. Y. Jackson, J. W. Jacobs, R. Sugaswara, S. H. Reich, P. A. Bartlett and P. G. Schultz, *J. Am. Chem. Soc.*, 1988, **110**, 4841.
3 D. Hilvert, S. H. Carpenter, K. D. Nared and M.-T. M. Auditor, *Proc. Natl. Acad. Sci. USA*, 1988, **85**, 4953.
4 U. Weiss and J. M. Edwards, *The Biosynthesis of Aromatic Amino Compounds*, Wiley, New York, 1980.
5 Y. M. Chook, J. V. Gray, H. Ke and W. N. Lipscomb, *J. Mol. Biol.*, 1994, **240**, 476.
6 Y. M. Chook, H. Ke and W. N. Lipscomb, *Proc. Natl. Acad. Sci. USA*, 1993, **90**, 8600.
7 M. R. Haynes, E. A. Stura, D. Hilvert and I. A. Wilson, *Science*, 1994, **263**, 646.
8 M. M. Davidson, I. R. Gould and I. H. Hillier, *J. Chem. Soc., Chem. Commun.*, 1995, 63.
9 O. Wiest and K. N. Houk, *J. Org. Chem.*, 1994, **59**, 7582.
10 M. M. Davidson and I. H. Hillier, *J. Chem. Soc., Perkin Trans. 2*, 1994, 1415.
11 M. M. Davidson and I. H. Hillier, *Chem. Phys. Lett.*, 1994, **225**, 293.
12 A. Y. Lee, P. A. Karplus, B. Ganem and J. Clardy, *J. Am. Chem. Soc.*, 1995, **117**, 3627.
13 Y. Xue, W. N. Lipscomb, R. Graf, G. Schnappauf and G. Braus, *Proc. Natl. Acad. Sci. USA*, 1994, **91**, 10 814.
14 M. J. Frisch, G. W. Trucks, M. Head-Gordon, P. M. W. Gill, M. W. Wong, J. B. Foresman, B. G. Johnson, H. B. Schlegel, M. A. Robb, E. S. Replogle, R. Gomperts, J. L. Andrés, K. Raghavachari, J. S. Binkley, C. Gonzalez, R. L. Martin, D. J. Fox, D. J. Defrees, J. Baker, J. J. P. Stewart and J. A. Pople, GAUSSIAN92, Gaussian, Inc., Pittsburgh, PA, 1992.
15 S. D. Copley and J. R. Knowles, *J. Am. Chem. Soc.*, 1987, **109**, 5008.
16 P. A. Bartlett and C. R. Johnson, *J. Am. Chem. Soc.*, 1985, **107**, 7792.
17 D. A. Pearlman, D. A. Case, J. C. Caldwell, G. L. Seibel, U. C. Singh, P. Weiner and P. A. Kollman, AMBER4.0, University of California, San Francisco, 1991.
18 S. J. Weiner, P. A. Kollman, D. A. Case, U. C. Singh, C. Ghio, G. Alagona, S. Profeta and P. Weiner, *J. Am. Chem. Soc.*, 1984, **106**, 765.
19 S. J. Weiner, P. A. Kollman, D. T. Nguyen and D. A. Case, *J. Comput. Chem.*, 1986, **7**, 230.
20 U. C. Singh and P. A. Kollman, *J. Comput. Chem.*, 1984, **5**, 129.
21 L. Pauling, *Chem. Eng. News*, 1946, **24**, 1375.
22 R. Wolfenden, *Annu. Rev. Biophys. Bioeng.*, 1976, **5**, 271.

23 G. R. Stark and P. A. Bartlett, *Pharmac. Ther.*, 1983, **23**, 45.
24 J. V. Gray and J. R. Knowles, *Biochemistry*, 1994, **33**, 9953.
25 J. V. Gray and D. Eren and J. R. Knowles, *Biochemistry*, 1990, **29**, 8872.
26 M. M. Davidson and I. H. Hillier, *J. Phys. Chem.*, 1995, **99**, 6748.
27 A. Fersht, *Enzyme Structure and Mechanism*, W. H. Freeman, New York, 2nd edn., 1985.
28 U. C. Singh and P. A. Kollman, *J. Comput. Chem.*, 1986, **7**, 718.
29 B. Waszkowycz, I. H. Hillier, N. Gensmantel and D. W. Payling, *J. Chem. Soc., Perkin Trans. 2*, 1991, 225.
30 A. Warshel and M. Levitt, *J. Mol. Biol.*, 1976, **103**, 227.
31 M. J. Field, P. A. Bash and M. Karplus, *J. Comput. Chem.*, 1990, **11**, 700.
32 J. Aqvist and A. Warshel, *Chem. Rev.*, 1993, **93**, 2523.
33 C. Gonzalez and H. B. Schlegel, *J. Chem. Phys.*, 1989, **90**, 2154.
34 R. J. Hall, M. M. Davidson, N. A. Burton and I. H. Hillier, *J. Phys. Chem.*, 1995, **99**, 921.
35 M. M. Davidson, I. H. Hillier and M. A. Vincent, *Chem. Phys. Lett.*, 1995, **246**, 536.
36 P. R. Andrews, G. D. Smith and I. G. Young, *Biochemistry*, 1973, **12**, 3492.
37 E. Brandes, P. A. Grieco and J. J. Gajewski, *J. Org. Chem.*, 1989, **54**, 515.
38 D. L. Severance and W. L. Jorgensen, *J. Am. Chem. Soc.*, 1992, **114**, 10 966.

Paper 5/06371J
Received 27*th September* 1995
Accepted 1*st December* 1995